PATULIN TRIGGERS NRF2-MEDIATED SURVIVAL MECHANISMS IN KIDNEY CELLS

Y. Pillay*, A. Phulukdaree[#], S. Nagiah*, A. A. Chuturgoon*

* Discipline of Medical Biochemistry, University of KwaZulu-Natal, Durban, South Africa

[#] Department of Physiology, University of Pretoria, Pretoria, South Africa

Address all correspondence to Prof Anil Chuturgoon, Discipline of Medical Biochemistry and Chemical Pathology, Faculty of Health Sciences, George Campbell Building, Howard College, University of KwaZulu-Natal, Durban, 4041, South Africa. Telephone: (031) 260 4404. Email: chutur@ukzn.ac.za

ABSTRACT

Patulin (PAT), a mycotoxin contaminant of apples and apple products, has been implicated in nephrotoxicity. PAT depletes glutathione (GSH) and elevates reactive oxygen species (ROS). The antioxidant (AO) response is activated by Nuclear erythroid 2-related factor (NRF2) and enhanced by Silent information regulator 3 (SIRT3). The effects of PAT on these molecules have yet to be examined. We investigated the effects of PAT on AO response survival pathways in human embryonic kidney cells (HEK293).

PAT cytotoxicity on HEK293 cells was evaluated (MTT assay; 24h; [0-100µM]) to determine an IC_{50}. GSH levels were measured using luminometry. Intracellular ROS was evaluated by flow cytometry. Protein expression of Keap1, NRF2, SIRT3 and PGC-1α was quantified by western blotting and gene expression of SOD2, CAT and GPx was evaluated by qPCR.

PAT caused a dose dependent decrease in HEK293 cell viability and a significant increase in levels of intracellular ROS (*p=0.0006*). A significant increase in protein expression (*p=0.029*)

was observed. PAT increased gene expression of SOD2 and CAT ($p=0.0043$), however, gene expression of GPx was significantly reduced ($p=0.0043$). These results show the up-regulation of NRF2 mediated AO mechanisms in response to PAT toxicity.

[1]1. INTRODUCTION

Patulin (PAT) is a mycotoxin produced by *Penicillium* and *Aspergillus* sp. (Liu, Wu et al. 2007). These moulds are common contaminants of apples and apple derived products. Several studies have identified PAT as a mutagen, teratogen and carcinogen with the liver and kidney as target organs (McKinley, Carlton et al. 1982, Zhou, Jiang et al. 2010).The kidneys metabolize and remove water soluble toxins from circulation (Ganong 2010). High renal blood flow, increased

---

[1] **Abbreviations:**

Patulin (PAT), reactive oxygen species (ROS), electron transport chain (ETC), antioxidant (AO), Glutathione (GSH), glutathione peroxidase (GPx), Nuclear erythroid 2-related factor (NRF2), AO response elements (ARE), Silent information regulator 3 (SIRT3), human embryonic kidney cells (HEK293), dimethyl sulphoxide (DMSO), 3-(4,5-Dimethyl-2-thiazolyl)-2,5-diphenyl-2H-tetrazolium bromide (MTT), phosphate buffer saline (PBS), complete culture medium (CCM), 2′,7′-dichlorodihydrofluorescein diacetate (H2DCF-DA), 2',7'-dichlorodihydrofluorescein (H2DCF), 2',7'-dichlorofluorescein (DCF), Mitochondrial membrane potential ($\Delta\psi_m$), Kelch-like ECH- associated protein (KEAP1), peroxisome proliferator-activated receptor-γ coactivator-1α (PGC1α), superoxide dismutase (SOD2)

toxin uptake, biotransformation and the concentrating ability of the kidney results in increased toxin exposure (Perazella 2009). PAT is a polar lactone that undergoes passive diffusion and active transport during renal elimination. The kidney is mitochondria rich to ensure a steady source of ATP for active removal of toxins (Ganong 2010). These high metabolic demands increases susceptibility to toxic insult through mitochondrial dysfunction and altered redox state (Perazella 2009).

Majority of cellular reactive oxygen species (ROS) is produced in the mitochondria during normal oxidative phosphorylation when electrons escape the electron transport chain (ETC) (Liu and Kamp 2011). ROS production is counteracted by cellular antioxidant (AO) systems which dampen ROS-mediated damage to macromolecules via detoxifying enzymes. This includes an array of biologically significant compounds specifically glutathione (GSH), glutathione peroxidase (GPx), superoxide dismutase (SOD) and catalase (CAT). Superoxide anions are commonly produced during cellular metabolism. The SOD2 isoform (Fe-MnSOD) located in the mitochondria catalytically detoxifies superoxide to molecular oxygen and hydrogen peroxide (Mates 2000). Hydrogen peroxide can be further detoxified to form water and molecular oxygen by CAT, a highly efficient ferritoprotoporphyrin-containing enzyme and GPx. The mitochondrial isoform of GPx is thus highly expressed in renal epithelial cells (Mates 2000, Dickinson and Forman 2002)

GSH, a thiol-containing compound, plays a pivotal role in the cellular defense system by reducing oxidative stress. GSH is used as a substrate by GPx for the reduction of hydroperoxides (Dickinson and Forman 2002). PAT is a strongly electrophilic molecule and exerts toxicity by covalently binding to protein thiol groups (Fliege and Metzler 1999). PAT binds strongly to GSH

and inhibits its AO function leading to elevated oxidative stress, oxidative DNA damage and cell death (Zhou, Jiang et al. 2010, Glaser and Stopper 2012).

When ROS generation exceeds the AO capacity, protein and DNA oxidation and lipid peroxidation ensue. Prevention of excessive oxidation in aerobic organisms is vital as depressed AO function leads to mutagenicity, cytotoxicity and carcinogenicity (Mates 2000). Nuclear erythroid 2-related factor (NRF2) regulates the expression of ROS detoxifying enzymes via the AO response elements (ARE). This transcription factor is implicated as a major defense mechanism against ROS mediated damage (Kansanen, Kuosmanen et al. 2013). Peroxisome proliferator-activated receptor-γ coactivator-1α (PGC1α) a transcriptional co-activator contributes to mitochondrial health and cell viability, signaling between the environment, mitochondrial biogenesis and AO expression. Silent information regulator 3 (SIRT3) is a mitochondrial NAD^{+}-dependent deacetylase located downstream of PGC1α which regulates several aspects of mitochondrial function including ATP generation, metabolism and mediation of the oxidative stress response (Cheng, Ren et al. 2013). NRF2, PGC1α and SIRT3 can be considered critical promoters of cell survival and mitochondrial function in response to oxidative stress.

Accumulating evidence of the adverse effects of PAT and the increased consumption of apple juice led to the establishment of a 50μg/l PAT safety level in apple juice (Sant'Ana, Rosenthal et al. 2008). Despite this regulation there are vast variations in PAT concentrations in apple products worldwide (Sant'Ana, Rosenthal et al. 2008). While several investigations assess the toxic effects of PAT in animal models, there is limited evidence for the molecular mechanisms for PAT-induced toxicity in humans. Recently however, studies have shown PAT is a potential initiator in skin tumorigenicity, shown both in mice and human keratinocytes. It is believed that

PAT below cytotoxic concentrations up-regulated survival mechanisms contributing the tumor initiation (Saxena, Ansari et al. 2011, Guo, Dong et al. 2013). Given the detoxification role of the kidney and high metabolic rates required, this organ may be susceptible to AO and ROS manipulation associated with cancer. Thus this study investigated the effects of PAT on AO response signaling in HEK293 cells.

2. MATERIALS AND METHODS:

Materials:

The HEK293 cell line was purchased from Highveld Biologicals (Johannesburg, South Africa (SA). All tissue culture reagents, the GSH-Glo[TM] Glutathione Assay, the Caspase-Glo® 3/7 Assay and ATP were obtained from Whitehead Scientific (Johannesburg, SA). The JC-1 dye and the 2′, 7′-dichlorodihydrofluorescein diacetate (H2DCF-DA) was purchased from BD Biosciences (Johannesburg, SA). Western blot reagents were purchased from Bio-Rad (Johannesburg, SA). qPCR primers were obtained from Inqaba Biotech. All other reagents were purchased from Merck (Johannesburg, SA) unless otherwise stated.

2.1 Cell culture

The HEK293 cells were cultured in Dulbucco's minimum essential medium supplemented with 1% L-glutamine, 1% penstrepfungizone, 10% fetal bovine serum and 2.5% HEPES. Cultures were maintained at 37°C with 5% CO_2. The 3-(4,5-Dimethyl-2-thiazolyl)-2,5-diphenyl-2H-tetrazolium bromide (MTT) assay was used to assess cell viability; cells were seeded into a 96-well microtitre plate, allowed to attach overnight and treated with PAT (0-100μM). For all

subsequent assays, cells were cultured to 90% confluency in 25cm^2 tissue flasks and treated with PAT.

2.2 Cell Viability Assay

Cell viability was determined using the MTT assay (Mosmann 1983). Approximately 20,000 cells (in six replicates) were exposed to a 0-100µM PAT range. After incubation with PAT for 24h, cells were washed twice with 0.1M phosphate buffer saline (PBS) and incubated with MTT salt solution (5 mg/ml in 0.1M PBS) and complete culture medium (CCM) (37°C, 4h). Thereafter, 100µl of dimethyl sulfoxide (DMSO) was added to each well and incubated (37°C, 1h) and the optical density was measured spectrophotometrically (Bio-tek µQuant; 570/690nm). The results were expressed as percentage cell viability vs. log concentration of PAT, from which the half maximal inhibitory concentration (IC$_{50}$) was determined. Cells were treated with the IC$_{50}$ (2.5µM) in all subsequent experiments. Control treatments were represented by an equal amount of DMSO solvent (0.0018%) in CCM without PAT.

2.3 Glutathione Assay

The GSH-Glo^{TM} Glutathione Assay (Promega, Madison, USA) was used to measure reduced GSH levels. PAT treated cells were transferred to an opaque microtitre plate (50µL of 20,000 cells/well; 6 replicates). GSH standards (0 – 5µM) were prepared from a 5mM stock solution diluted in deionized water. Five two-fold dilutions of the GSH stock were prepared and transferred into wells (50µL) of the microtitre plate. The 2X GSH-Glo^{TM} Reagents were prepared according to the manufacturer's instructions, added to the experimental wells (50µL/well), and incubated at room temperature (RT, 30min). Reconstituted Luciferin Detection Reagent (50µL) was added to each well and incubated (RT, 15min) before the luminescence was

measured (Modulus^{TM} microplate luminometer, Turner Biosystems, Sunnyvale, USA). A standard curve was derived and the GSH concentration in each sample was extrapolated from the equation (y= 762884.78x + 143767.87; R^2=1.00).

2.4 DCF Assay

The level of intracellular ROS (O$_2^{\bullet-}$, hydrogen peroxide, peroxynitrite) in HEK293 cells was quantified by fluorescence activated cell sorting (FACS) with the fluorescent probe, H2DCF-DA. Intracellular ROS oxidize H2DCF-DA to 2', 7'-dichlorofluorescein (DCF) which emits fluorescence at 525nm. Briefly, treated cells (1 × 10^6) were incubated in phenol red-free media supplemented with 10% fetal calf serum and 10μM H2DCF-DA for 45 min at 37°C. Cells were then rinsed thrice with 0.1M PBS (400 x g, 5min, RT). Stained cells were resuspended in 150μl of 0.1M PBS and analysed using the Accuri^{TM} C6 flow cytometer (BD Bio). Events were gated and the fluorescence measured on FL-1 channel (525nm) of the Accuri^{TM} C6 flow cytometer (Becton Dickinson). A total of 20 000 events were acquired and analysed using the CFlow Plus Software.

2.5 Quantitative PCR

2.5.1 cDNA preparation

RNA was isolated from cells in 25cm^2 flasks with TriReagent as per protocol. Briefly, 500μl Trizol was added to 500μl cells (2.5x10^6 in 0.1M PBS) incubated for 1h at -80°C. Chloroform (100μl) then was added and centrifuged at (12,000xg, 15min, 4°C) followed by the addition of propan-2-ol (250μl, 1h, -80°C) before centrifugation (12,000xg, 20min, 4°C). Samples were then washed with 500μl cold ethanol (75%) and centrifuged (7,400xg, 15min, 4°C). Following the removal of ethanol, RNA pellets were resuspended in 15µl nuclease-free water, quantified

(Nanodrop2000) and standardised 2,000ng/µl. A 20µl reaction volume containing 1µl RNA template, 4µl 5X iScript™ reaction mix, 1µl iScript reverse transcriptase and nuclease free water was used to synthesise cDNA (iScript™ cDNA Synthesis kit (BioRad; catalogue no 107-8890). Thermocycler conditions were 25°C for 5min, 42°C for 30min, 85°C for 5min and a final hold at 4°C.

2.5.2 Quantitative PCR

Gene expression of superoxide dismutase (SOD2) [Sense 5'GAGATGTTACACGCCCAGA TAGC-3'; Antisense 5-AATCCCCAGCAGTGGAATAAGG-3'(57˚C)], Catalase (CAT) [Sense 5'-TAAGACTGACCAGGGCATC-3'; Antisense 5'-CAACCTTGGTGAGATCGAA-3'(58˚C)] and GPx [Sense 5'-GACTACACCCAGATGAACGAGC-3'; Antisense 5'-CCCACCAGGAA CTTCTCAAAG-3'(58˚C)] were evaluated using the iQ™ SYBR® Green PCR kit (BioRad; 170-880). Briefly, 2.5 µl cDNA template, 30nM sense primer, 30nM antisense primer, 5X iScript reaction mix and nuclease free water was made up to a reaction volume of 25µl. All assays were carried out using CFX Touch™ Real Time PCR Detection System (BioRad). The reaction was subjected to initial denaturation (95˚C, 4min), followed by 37 denaturation cycles (95˚C, 15sec), annealing (primer-specific temperature, 40sec), extension (72˚C, 30sec) and a plate read for 37 cycles. β actin was run under the same conditions and used as the housekeeping gene. Data was analysed using the method described by Livak and Schmittgen represented as fold change ($2^{-\Delta\Delta CT}$) relative to the housekeeping gene, actin [Sense 5'-TGACGGGTCACCCACACTGTGCCCAT-3'; β Actin – Antisense 5'-CTAGAAGCATTTGCGGTGGACGATGGAGGG-3'] and control (Livak and Schmittgen 2001).

2.10 Western Blotting

Cytobuster™ reagent (Novagen, Pretoria, SA), supplemented with protease and phosphatase inhibitors (Roche, 05892791001 and 04906837001, respectively) was used for protein isolation. Cytobuster (200µl) was added to the cells (4°C, 10min) and centrifuged (180 x g; 4°C, 10min) to obtain crude protein extracts. Protein samples were quantified using the bichinchoninic assay and standardized (1mg/ml). Samples (25µl) were electrophoresed on 7.5% sodium dodecyl sulfide-polyacrylamide electrophoresis gels and electro-transferred to nitrocellulose membranes. Membranes were blocked with 3% bovine serum albumin (BSA) in Tris buffer saline (20mM Tris–HCl; pH 7.4), 500mM NaCl and 0,01% Tween 20; TBST) for 1h, and incubated with primary antibody (NRF2, CS 8882; Kelch-like ECH- associated protein (Keap1), CS80475; PGC1α, CS2178; (Cell Signaling, Danvers, USA) SIRT3, AB86671; (Abcam, Pretoria, South Africa) β Actin, A3854 (Sigma-Aldrich, Johannesburg, SA); 1:1000 dilution in 1% BSA in TTBS) at 4°C overnight. Membranes were washed five times (10ml TBST, 10min) and treated with horseradish peroxidase-conjugated secondary antibody (rabbit, sc-2054; mouse, ab97046; 1:10,000) (1h, RT). Membranes were washed 3 times (TBST, 15min) and immunoreactivity was detected (Clarity Western ECL Substrate) with the Uvitech Image Documentation System (UViTech Alliance 2.7). Protein bands were analyzed with the UViBand Advanced Image Analysis software (UViTech v12.14) and normalized against the corresponding β Actin bands. Results are reported as relative band density.

Statistical Analysis

Statistical evaluation was completed using GraphPad PRISM® v5.00. Statistical significance was set at 0.05 and comparisons were made using unpaired t tests with Welch correction.

3. RESULTS

3.1 Cell Viability

The MTT assay showed that PAT at a concentration of 100µM decreased viability to 2% in HEK293 cells and an IC_{50} of 2.5µM was determined (Fig 1). This concentration was used in all subsequent experiments.
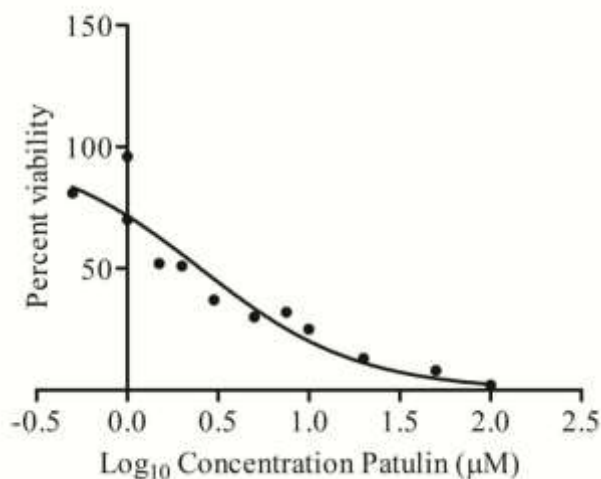

Figure 1. Patulin induced a dose dependent decrease in HEK293 cell viability.

3.2 Oxidative stress

The effect of PAT on endogenous cellular GSH concentrations was examined. PAT significantly depleted GSH (3.67 ± 0.11µM) compared to untreated cells (7.41 ± 0.20µM; *p=0.0048;* Fig 2A). We then investigated the effect of PAT on intracellular superoxide production. Intracellular superoxide levels were markedly raised by 54.7% (99.04 ± 0.29%) in PAT treated cells compared to the control (44.34 ± 1.20%; *p=0.0006*; Fig 2B).
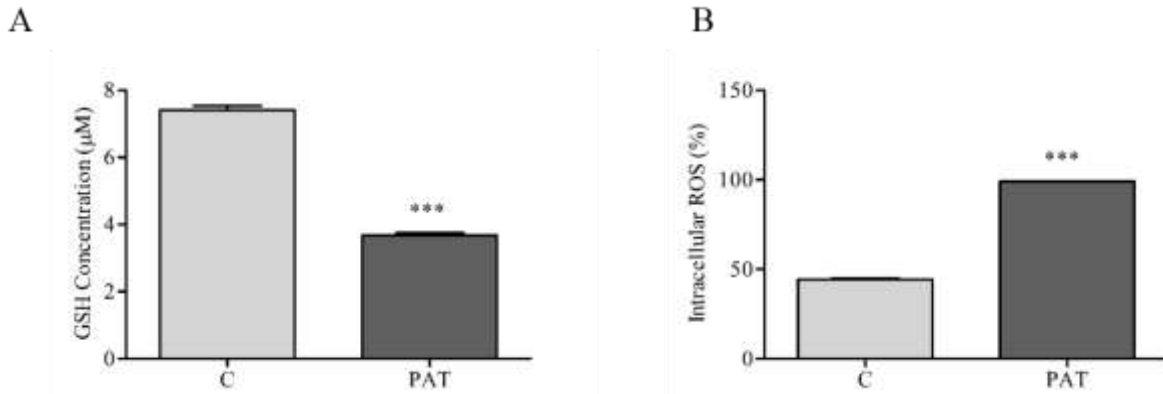
Figure 2. Patulin (2.5μM) depleted glutathione and increased reactive oxygen species production in HEK293 cells after 24h exposure. A) Luminometry showed PAT decreased GSH concentration (*p=0.0048*) B) The DCF assay indicated elevated intracellular superoxide levels in PAT treated protein expression in PAT treatments (*p=0.0006*).

3.3 Antioxidant Survival Mechanisms

A 1.5-fold increase in NRF2 protein expression (1.52 ± 0.25 relative to normalized control 1.00 ± 0.01; *p=0.029*; Fig 3A) was observed with an associated -1.3 fold decrease in Keap1 levels (-1.325 ± 0.55 relative to normalized control 1.00 ± 0.01; *p=0.029*; Fig 3A). The associated AO gene expression was significantly elevated with respect to CAT (6.26 ± 0.65 relative to normalized control 1.00 ± 0.00; *p=0.0043;* Fig 3B) and SOD2 (11.92 ± 3.19 relative to normalized control 1.00 ± 0.00; *p=0.0043;* Fig 3B). GPx activity however, was suppressed (-1.47 ± 0.35 relative to normalized control 1.00 ± 0.00; *p=0.0043;* Fig 3B). The analysis for mitochondrial signaling molecules SIRT3 (1.28 ± 0.12 relative to normalized control 1.00 ± 0.01; *p=0.029;* Fig 3B) and PGC1α (1.25 ± 0.17 relative to normalized control 1.00 ± 0.01; *p=0.029;* Fig 3A) indicated elevated protein expression in PAT treated cells (Fig 3A).
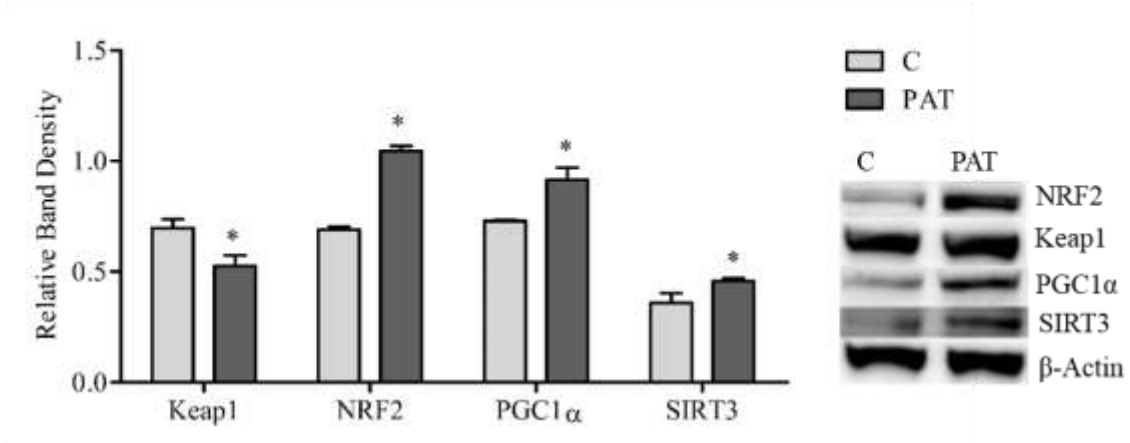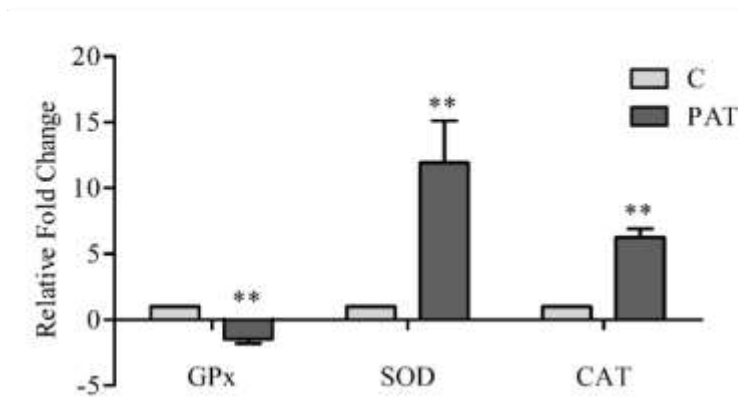
Figure 3. **Patulin altered the antioxidant response in HEK293 cells at 24h.** A) Western Blotting densitometric analysis showed significantly increased levels of NRF2 *(p=0.029)*, Keap1 *(p=0.029)*, PGC1α *(p=0.029)* and SIRT3 *(p=0.029)*.B) qPCR determination of AO gene expression showing: elevated SOD2 *(p=0.0043)* and CAT *(p=0.0043)* with a decrease in GPx *(p=0.0043)*, compared to the control.

4. DISCUSSION:

The high affinity of sulfhydryl binding by PAT and associated oxidative stress due to GSH depletion has been reported in both *in vitro* and *in vivo* models (McKinley, Carlton et al. 1982, Zhou, Jiang et al. 2010). There is limited evidence, however, on the mechanism of activation of the AO response pathways by PAT in kidney cells.

Our findings of GSH depletion and diminished GPx activity are in agreement with the study conducted by Fliege and Metzler (1999) (Fliege and Metzler 1999). We also found a corresponding increase in ROS levels. An imbalance in intracellular antioxidant and oxidant levels promotes ROS-mediated damage to macromolecules (Zhou, Jiang et al. 2010). However, innate cellular mechanisms are effected in an attempt to maintain redox homeostasis. One such mechanism includes the Keap1/NRF2 signaling pathway (Kansanen, Kuosmanen et al. 2013). Under basal conditions, NRF2 is anchored to cysteine-rich Keap1 in the cytosol, marking NRF2 for proteosomal degradation. Intracellular increases in ROS and electrophilic substances such as PAT, modify the cysteine residues on Keap1 causing a conformational change that triggers the release of NRF2 (Kansanen, Kuosmanen et al. 2013). The accumulating NRF2 translocates to the nucleus and binds to ARE to elevate transcription of AO stress proteins (Kansanen, Kuosmanen et al. 2013). Protein analysis showed PAT caused a 1.5 fold elevation in NRF2 and a concomitant decrease in Keap1, thus increasing levels of unbound NRF2. These novel findings may further support the toxic relationship between PAT and thiol-containing GSH depletion (Bryan, Olayanju et al. 2013). NRF2 also regulates the utilization and regeneration of GSH (Harvey, Thimmulappa et al. 2009). The observed increase in NRF2 may be a compensatory mechanism to replenish GSH depletion and up-regulate associated AO enzymes. Furthermore,

we found an up regulation of NRF2, and corresponding increase in transcription of detoxifying enzymes, SOD2 and CAT (Fig 3B); in agreement with Liu et al. (2007) (Liu, Wu et al. 2007).

Transcriptional co-activator, PGC1α, a potent regulator of cellular metabolism, maintains the balance between the production and scavenging of oxidants by controlling mitochondrial biogenesis and AO gene expression (Vazquez, Lim et al. 2013). PAT significantly up-regulated PGC1α levels, which has been shown to induce SOD2 and GPx gene expression to reduce mitochondrial ROS (St-Pierre, Drori et al. 2006, Vazquez, Lim et al. 2013).

PGC1α has also been shown to stimulate SIRT3 gene expression. SIRT 3 controls NAD^+ dependent mitochondrial substrate deacetylation and attenuates ROS by deacetylating and activating SOD2 and CAT ultimately augmenting the production of these enzymes via interactions with Foxo3a in response to oxidative stress (Kong, Wang et al. 2010, Verdin, Hirschey et al. 2010, Zhong and Mostoslavsky 2011). This is the first study to corroborate these findings showing significant increases in protein expression (Fig 2) and concomitant increases in AO gene expression (Fig 3) (St-Pierre, Drori et al. 2006, Kong, Wang et al. 2010, Vazquez, Lim et al. 2013). GPx, however, requires GSH as a substrate for hydroperoxide detoxification hence remained unaffected in spite of PGC1α and SIRT3 activation (Fig 3). Similar effects on GPx were observed in a recent study on deoxynivalenol induced toxicity in HepG2 cells (Mishra, Dwivedi et al. 2014).

CONCLUSION

Exposure to PAT caused a decrease in the cells antioxidant capacity as noted by depleted intracellular GSH and a corresponding increase in intracellular ROS. The innate cell survival mechanisms to adapt to oxidative stress was activated following PAT exposure via the up-

regulation of AO transcription factors, NRF2 and PGC1α; and AO gene expression, SOD, CAT, GPx and SIRT3 in HEK293 cells.

CONFLICT OF INTEREST

None declared.

REFERENCES

Bryan, H. K., A. Olayanju, C. E. Goldring and B. K. Park (2013). "The Nrf2 cell defence pathway: Keap1-dependent and-independent mechanisms of regulation." Biochemical Pharmacology **85**(6): 705-717.

Cheng, Y., X. Ren, A. S. Gowda, Y. Shan, L. Zhang, Y. Yuan, R. Patel, H. Wu, K. Huber-Keener and J. Yang (2013). "Interaction of Sirt3 with OGG1 contributes to repair of mitochondrial DNA and protects from apoptotic cell death under oxidative stress." Cell Death & Disease **4**(7): e731.

Dickinson, D. A. and H. J. Forman (2002). "Glutathione in defense and signaling." Annals of the New York Academy of Sciences **973**(1): 488-504.

Fliege, R. and M. Metzler (1999). "The mycotoxin patulin induces intra- and intermolecular protein crosslinks in vitro involving cysteine, lysine, and histidine side chains, and alpha-amino groups." Chemico-Biological Interactions **123**(2): 85-103.

Ganong, F., Barrett, K.E., Barman, S.M., Boitano, S., Brooks, H.L., (2010). Ganong's Review of Medical Physiology, Twenty-Third Edition. United States of America, McGraw-Hill Companies, Inc. .

Glaser, N. and H. Stopper (2012). "Patulin: Mechanism of genotoxicity." Food and Chemical Toxicology **50**(5): 1796-1801.

Guo, X., Y. Dong, S. Yin, C. Zhao, Y. Huo, L. Fan and H. Hu (2013). "Patulin induces pro-survival functions via autophagy inhibition and p62 accumulation." Cell Death & Disease **4**: e822.

Harvey, C., R. Thimmulappa, A. Singh, D. Blake, G. Ling, N. Wakabayashi, J. Fujii, A. Myers and S. Biswal (2009). "Nrf2-regulated glutathione recycling independent of biosynthesis is critical for cell survival during oxidative stress." Free Radical Biology and Medicine **46**(4): 443-453.

Kansanen, E., S. M. Kuosmanen, H. Leinonen and A.-L. Levonen (2013). "The Keap1-Nrf2 pathway: Mechanisms of activation and dysregulation in cancer." Redox Biology **1**(1): 45-49.

Kong, X., R. Wang, Y. Xue, X. Liu, H. Zhang, Y. Chen, F. Fang and Y. Chang (2010). "Sirtuin 3, a new target of PGC-1α, plays an important role in the suppression of ROS and mitochondrial biogenesis." PloS one **5**(7): e11707.

Liu, B.-H., T.-S. Wu, F.-Y. Yu and C.-C. Su (2007). "Induction of oxidative stress response by the mycotoxin patulin in mammalian cells." Toxicological Sciences **95**(2): 340-347.

Liu, G. and D. W. Kamp (2011). "Mitochondrial DNA Damage: Role of Ogg1 and Aconitase."

Livak, K. J. and T. D. Schmittgen (2001). "Analysis of relative gene expression data using real-time quantitative PCR and the 2(-Delta Delta C(T)) Method." Methods **25**(4): 402-408.

Mates, J. M. (2000). "Effects of antioxidant enzymes in the molecular control of reactive oxygen species toxicology." Toxicology **153**(1-3): 83-104.

McKinley, E. R., W. W. Carlton and G. D. Boon (1982). "Patulin mycotoxicosis in the rat: toxicology, pathology and clinical pathology." Food and Chemical Toxicology **20**(3): 289-300.

Mishra, S., P. D. Dwivedi, H. P. Pandey and M. Das (2014). "Role of oxidative stress in Deoxynivalenol induced toxicity." Food and Chemical Toxicology **72**: 20-29.

Mosmann, T. (1983). "Rapid colorimetric assay for cellular growth and survival: Application to proliferation and cytotoxicity assays." Journal of Immunological Methods **65**(1–2): 55-63.

Perazella, M. A. (2009). "Renal vulnerability to drug toxicity." Clinical Journal of the American Society of Nephrology **4**(7): 1275-1283.

Sant'Ana, A. d. S., A. Rosenthal and P. R. de Massaguer (2008). "The fate of patulin in apple juice processing: A review." Food Research International **41**(5): 441-453.

Saxena, N., K. M. Ansari, R. Kumar, B. P. Chaudhari, P. D. Dwivedi and M. Das (2011). "Role of mitogen activated protein kinases in skin tumorigenicity of patulin." Toxicology and Applied Pharmacology **257**(2): 264-271.

St-Pierre, J., S. Drori, M. Uldry, J. M. Silvaggi, J. Rhee, S. Jäger, C. Handschin, K. Zheng, J. Lin and W. Yang (2006). "Suppression of reactive oxygen species and neurodegeneration by the PGC-1 transcriptional coactivators." Cell **127**(2): 397-408.

Vazquez, F., J.-H. Lim, H. Chim, K. Bhalla, G. Girnun, K. Pierce, C. B. Clish, S. R. Granter, H. R. Widlund and B. M. Spiegelman (2013). "PGC1α expression defines a subset of human melanoma tumors with increased mitochondrial capacity and resistance to oxidative stress." Cancer Cell **23**(3): 287-301.

Verdin, E., M. D. Hirschey, L. W. Finley and M. C. Haigis (2010). "Sirtuin regulation of mitochondria: energy production, apoptosis, and signaling." <u>Trends in Biochemical Sciences</u> **35**(12): 669-675.

Zhong, L. and R. Mostoslavsky (2011). "Fine tuning our cellular factories: sirtuins in mitochondrial biology." <u>Cell Metabolism</u> **13**(6): 621-626.

Zhou, S.-m., L.-p. Jiang, C.-y. Geng, J. Cao and L.-f. Zhong (2010). "Patulin-induced oxidative DNA damage and p53 modulation in HepG2 cells." <u>Toxicon</u> **55**(2): 390-395.